

Ground Penetrating Radar Utilizing Compressive Sampling and OFDM Techniques

Mohamed Metwally, Nikolai L'Esperance, and Tian Xia
School of Engineering, University of Vermont
Burlington, Vermont, United States

Abstract—In this paper, we propose a new GPR design method by combining OFDM (Orthogonal Frequency Division Multiplexing) and compressive sampling (CS) techniques. Comparing with traditional SFCW (step frequency continuous wave) radar, OFDM allows transmitting/receiving multiple frequency tones simultaneously to reduce frequency sweeping time. Compressive sampling reduces the number of frequency tones required to further improve GPR operating efficiency. To show the design effectiveness, SFCW GPR and OFDM-CS continuous wave GPR are both simulated in conjunction with FDTD (finite difference time domain) numerical modeling to characterize a concrete slab model.

Index Terms—Compressive Sampling, GPR, OFDM, SFCW, Radar

I. INTRODUCTION

As a non-destructive sensing technique, ground penetrating radar (GPR) has received great attentions recently for its capability of performing subsurface structural inspections. One major application domain is transportation infrastructures, such as bridge deck or roadway pavement structural quality and safety assessment.

GPR is typically designed with two different approaches. The first is the impulse radar (IR) design [1, 2], where pulse signals are produced to penetrate through the medium under inspection, and echoes are received and analyzed for structural characterizations. The pulse width is usually very narrow, i.e. ~ 1 ns, resulting in an ultra-wide frequency bandwidth. The IR design has simple circuit architecture as the baseband pulses are transmitted directly. Drawbacks of IR sensing feature low dynamic range and the requirement of high speed high resolution ADC, which greatly increase design cost and complexity.

A second approach is the continuous wave (CW) radar where a primary architecture is stepped frequency continuous wave (SFCW) radar [3, 4]. SFCW radar does not transmit a pulse signal in the traditional manner, but rather synthesizes the effect of pulse transmission and detection. It decomposes a pulse signal into frequency spectrum components, then sequentially transmits a sinusoidal signal of each individual frequency, and measures the corresponding echo. At every frequency, the phase and amplitude gain responses from the scatter are recorded. Once responses at all frequencies are measured, they will be assembled into a matrix to perform inverse Fourier transform to synthesize the time domain impulse response for scatter characterizations. Since SFCW radar operates across the same frequency band as an impulse system, it yields essentially the equivalent characterizations while with more advantages: An SFCW system does not require a high speed ADC for data acquisition. Different waveforms can be easily synthesized through spectrum manipulation for leveraging sensing performance under

various conditions. Also it can easily bypass frequencies that have strong interferences.

The main weakness of SFCW radar is associated with its relatively low sensing speed. Since different frequency tones are emitted individually and sequentially, for a large number of frequency tones, it takes a long time to complete the full spectrum frequency sweeping. Also if the relative positions between the object under test and radar are fast moving, the low frequency sweeping speed may not very well keep up with object state varying. As a result, the radar image might be smeared and radar radial-velocity sensing sensitivity could be degraded. To solve this problem, we propose to develop OFDM technique so that multiple frequency tones can be generated and emitted simultaneously. By making different frequency tones orthogonal to each other, their cross interferences are minimized. In GPR subsurface sensing, the potential targets generally cover a small part of the total subsurface volume [4]. Taking advantage of this spatial sparsity property, compressive sampling can be employed to reduce the number of frequency tones for OFDM signal generation without compromising sensing accuracy. With OFDM and CS integration, GPR sensing efficiency can be leveraged.

The paper is organized as below: Section 2 introduces OFDM and compressive sensing techniques. Section 3 describes FDTD method for channel modeling. Section 4 shows simulation results. The concluding remarks and future work are presented in section 5.

II. OFDM THEORY AND COMPRESSIVE SAMPLING

2.1 Orthogonal Frequency Division Multiplexing

OFDM is a well-known spread spectrum technique widely used in modern communication systems to achieve high data rates and to alleviate multi-path effects. In this study, OFDM technique is adapted for radar signal generation [5, 6, 11], where multiple frequency tones are generated and transmitted simultaneously. As different frequency tones are orthogonal among each, their cross-interferences are minimized. Comparing with sequential frequency tone generation in SFCW radar, OFDM technique can accelerate radar operating speed.

Inverse Digital Fourier Transform (IDFT) has been proven to be a cost effective approach for multi-tone OFDM signal generation [5, 6]. To produce N frequency tones, N coded data X_k ($k=0,1,\dots,N-1$) are used as IDFT inputs defining signal spectrum. With the sampling frequency F_s and the sampling time instance $t = nT_s = n/F_s$, the IDFT can be expressed as:

$$x(nT_s) = \frac{1}{N} \sum_{k=0}^{N-1} X_k e^{j2\pi k f_a n T_s}. \quad (1)$$

where $x(nT_s)$ is the time domain sampling data point, f_a specifies frequency spacing between two adjacent tones. When F_s equals N times the frequency spacing f_a , the

orthogonality among different tones is ensured [5]. In other words, the inter-tone interference is eliminated, which is illustrated in Fig. 1.

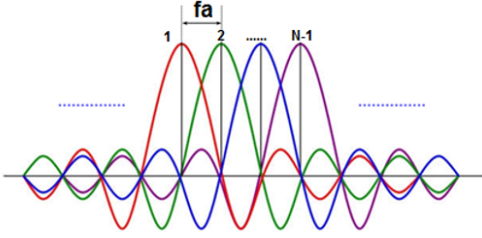


Fig. 1. Frequency spectrum of an N-tone OFDM signal

The X_k coding is based on a selected digital modulation scheme. There are two major types of digital modulation schemes: M-ary phase shift keying (M-PSK) and M-ary quadrature amplitude modulation (M-QAM). In this design, Quadrature PSK (QPSK) is utilized such that X_k symbol magnitudes are made equal while their phases are randomized. As a result, OFDM time domain signal produces a high signal to noise ratio (SNR). The detailed explanation can be found in our other publications [6, 11].

2.2 COMPRESSIVE SAMPLING

Compressive sampling is a novel data encode/decode theory utilizing sparsity and compressibility of a signal [7, 8, 9]. Distinct from the classic Nyquist sampling, CS focuses on the “information” carried by a signal itself. In CS framework, it has been shown that a signal, which is sparse in some basis, can be captured from a small number of random non-adaptive linear projections onto the measurement basis. The original signal can be reconstructed with incomplete measurement data through linear optimization. The capability of CS provides a new perspective for radar sensing data reduction without compromising the sensing quality.

Considering a signal $x \in \mathbb{R}^N$, it is K sparse if it can be represented in a domain by K coefficients, where $K < N$. Such representation can be achieved using an orthogonal transform matrix Ψ that is able to convert the signal into K dominant coefficients in a different domain, which can be portrayed as follows [8]

$$x = \Psi\theta \quad (2)$$

where Ψ is the sparsity transform and θ is a $N \times 1$ vector with K nonzero elements. According to the theory of CS, if the signal x is sparse in a basis, the measurement vector of x can be expressed as

$$y^{M \times 1} = \Phi^{M \times N} x^{N \times 1} = \Phi^{M \times N} \Psi^{N \times N} \theta^{N \times 1}, \quad (3)$$

where Φ represents a $M \times N$ measurement matrix, and M ($K < M \ll N$) denotes the number of measurements. CS theory stipulates that if $\Phi^{M \times N} \Psi^{N \times N}$ possesses the restricted isometry property (RIP) [10], then it is possible to recover the signal x from the compressed measurement vector y by solving the ℓ_1 optimization problem as follows:

$$\theta = \arg \min \|\theta\|_1, \quad s. t. \quad y = \Phi\Psi\theta \quad (4)$$

To ensure RIP, it is imperative to have a high measure of incoherence between $\Phi^{M \times N}$ and $\Psi^{N \times N}$. Findings in compressive sensing [10] indicate that a general random basis has a high degree of incoherence with any basis [12]. Hence, a random matrix can be chosen to be the projection basis $\Phi^{M \times N}$.

In GPR application, as the target space is generally sparse, a random subset of M frequencies can be utilized for SFCW radar sensing operation [4, 14]. In this design, we utilize M frequency tones for OFDM signal generation and transmission. Employing such reduced set of frequencies with CS reduces the test signal power consumption and test signal complexity.

III. STRUCTURAL FDTD MODELING

For validation purposes, we carry out GPR functional simulations with a mock-up bridge deck segment shown in Fig. 2. SFCW GPR and OFDM-MCS GPR signals will be generated respectively to scan the structure and results will be compared. The bridge deck segment emulates a concrete slab covered with a hot-mix asphalt layer, and a rebar is buried inside the concrete layer. The top side and bottom side air layers are 36 cm and 3.9 cm thick. Other parameter values are illustrated in the figure.

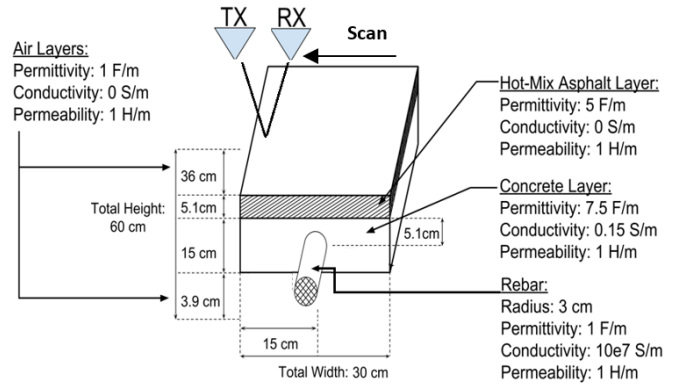


Fig. 2. Bridge deck concrete slab model

A 2D Finite Difference Time Domain (FDTD) method is employed to develop the computational model characterizing GPR signal propagation in the concrete slab. FDTD is a grid-based differential numerical modeling method that discretizes Maxwell’s equations using central-difference approximations to the space and time partial derivatives. In this study, the transverse electric (TE) mode is adopted, and perfectly matched layer (PML) absorbing boundaries model is applied to eliminate reflections from the edges of the modeling grid. The governing TE mode field equations are:

$$\frac{\partial E_x}{\partial t} = \frac{1}{\epsilon} \left(\frac{\delta H_z}{\delta y} - \sigma E_x \right) \quad (5)$$

$$\frac{\partial E_y}{\partial t} = \frac{1}{\epsilon} \left(\frac{\delta H_z}{\delta x} - \sigma E_y \right) \quad (6)$$

$$\frac{\partial H_z}{\partial t} = \frac{1}{\mu} \left(\frac{\delta E_x}{\delta y} - \frac{\delta E_y}{\delta x} - \frac{\delta \mu}{\epsilon} H_z \right) \quad (7)$$

where E_x are E_y are transverse electrical field components and H_z is the longitudinal magnetic field component. ϵ , σ and μ specify medium’s permittivity, conductivity and permeability respectively. Their values for different mediums are provided in Fig. 2.

To compute the electrical field and the magnetic field, Yee scheme [12] is applied to discretize, both in time and space, the above TE mode governing equations with central difference approximations. In our simulations, the GPR test signal is generated with 800 MHz bandwidth. In order to achieve fine resolution and accuracy, we choose 1 GHz as the maximum frequency to set the FDTD spatial increment Δx as

3 mm, which produces 100 samples per wavelength at high end of the excitation spectrum. While the temporal step is computed correspondingly as $\Delta t = \Delta x / (2C) = 5$ ps to ensure the stability condition. C is the light speed in air.

IV EXPERIMENTAL SIMULATIONS

4.1 A-scan Simulations

For the test validation, GPR A-scan simulations with SFCW and OFDM-CS approaches are performed. The A-scan is a stationary measurement from a specific position, where the transmitter and receiver antennas are fixed at a location to radiate source signals, receive the echoes and synthesize the response pulses. In both approaches, radar signals are generated with the same bandwidth of 800 MHz. For SFCW, 1024 sinusoidal signals are emitted sequentially to the concrete slab. The frequency step size is 781.25 kHz. The source signal spectrum envelop is designed as Fig. 3b shows, and the corresponding synthesized time domain Gaussian pulse is depicted in Fig. 3a. The FDTD analysis is performed to characterize the channel (concrete slab) response under each individual frequency, and the respective magnitude and phase responses are extracted and recorded in succession. After testing all frequency tones, all magnitude and phase response data are assembled in a matrix. By carrying out the inverse DFT calculation, the time domain A-scan response waveform is obtained, shown in Fig. 3d.

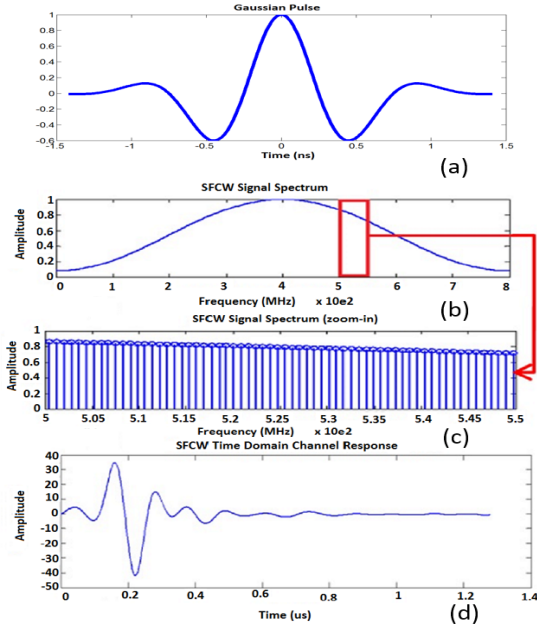


Fig. 3 (a) Synthesized time domain Gaussian pulse; (b) SFCW transmission signal spectrum (c) zoom-in view of spectrum segment (d) Synthesized A-scan reflection waveform

For OFDM-CS A-scan simulation, the algorithm is set up to randomly pick M frequency tones for OFDM signal generation. For those unselected tones, their amplitudes are set to be zero. The signal spectrum is shown in Fig. 4a, and Fig. 4b is a zoomed-in view of a segment. The scatter reflection signal is analyzed to characterize scatter response, where magnitude and phase responses corresponding to M selected frequency tones are extracted. Convex programming algorithm

[7, 8, 9] is then utilized to recover the full spectrum response. In this case, the magnitude and phase responses of 1024 frequency tones. To synthesize the time domain A-scan waveform, inverse Fourier transform is conducted. Fig. 4c depicts OFDM-CS analysis result, where the A-scan response pulse waveform is restructured from $M=600$ frequency tones.

To evaluate OFDM-CS algorithm performance, two quantitative metrics are employed, which are cross-correlation and signal-error ratio (SER).

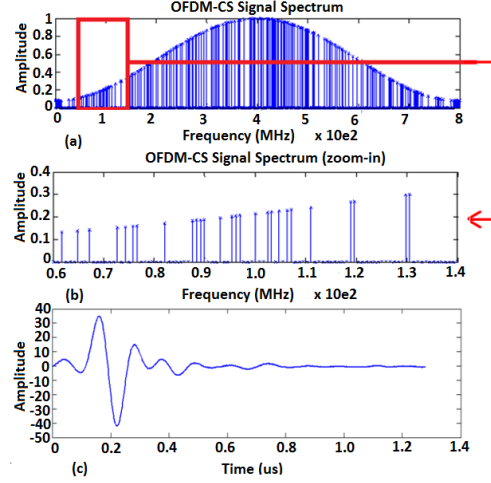


Fig. 4 (a) OFDM-CS signal spectrum (600 tones) (b) zoom-in view of spectrum segment (c) Synthesized A-scan response waveform

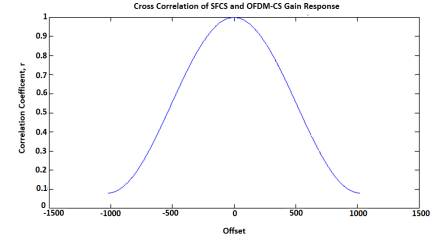


Fig. 5. Cross correlation of SFCW and OFDM-CS Gain responses

Fig. 5 depicts the cross correlation between OFDM-CS response data and SFCW response data. As can be observed, the cross correlation coefficient peaks at 0.9991, which indicates a good similarity between OFDM-CS and SFCW testing results.

The SER measures how identical the results obtained from two approaches are. The SER computation equation is:

$$SER = 10 \log_{10} \left[\frac{\sum_{i=1}^{1024} X_i^2}{\sum_{i=1}^{1024} (X_i - Y_i)^2} \right] \quad (8)$$

where X_i is the i^{th} frequency tone response reconstructed with OFDM-CS approach, while Y_i is the i^{th} frequency tone response measured with SFCW method. The SER value for $M = 600$ is calculated to be 27.0 dB.

Table 1. A-Scan Test metrics for different compression ratios

M Frequency Tones	Compression Ratio	SER (dB)	Cross-Correlation
1000	1.02X	71.4	1.0000
800	1.28X	37.1	0.9999
600	1.71X	27.0	0.9991
400	2.56X	21.3	0.9965
200	5.12X	10.8	0.9601
100	10.2X	5.8	0.8643

For further examination, more A-scan experiments are performed with different compression ratios. Results are tabulated in Table 1.

4.2. B-scan Simulations

In this part of study, GPR B-scan simulations are conducted, where the transmitter and receiver antennas are moved to scan the whole concrete slab area. As antennas change to each new location, the A-scan reflection waveform is collected and recorded in a matrix. At the end of the scan process, the matrix recording all A-scan data is used to assemble a 2-dimensional (2D) image illustrating the cross-sectional view, which produces the B-scan image.

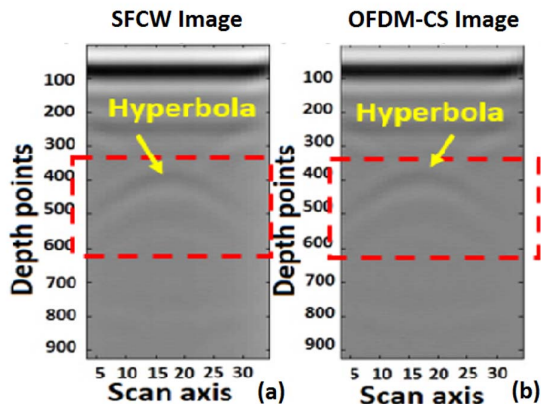


Fig. 6. a) SFCW B-scan image; b) OFDM-CS B-scan image obtained with 600 frequency tones

For performance evaluation, B-scan images are produced employing both SFCW approach and OFDM-CS approach. Fig. 6a shows the SFCW image obtained with 1024 frequency tones, while Fig. 6b is the OFDM-CS image reconstructed from using 600 frequency tones. In both images, the signature hyperbola pattern corresponding to the buried rebar [15] can be effectively detected. To gauge the degree of images similarity, a 2D cross-correlation is computed. For the above two images, the maximum correlation coefficient is 0.9508. We also calculate OFDM-CS B-scan image SER using SFCW image as the reference. The resulting SER equals 21.23dB.

The OFDM-CS B-scan experiments are further repeated under other compression ratios. Cross-correlation and SER results are computed and illustrated in Fig. 7 and Fig. 8 respectively.

IV. CONCLUSION AND FUTURE WORK

A new approach combining OFDM and compressive sampling is developed for continuous wave GPR system design. Simulations have been performed showing that OFDM-CS is able to achieve comparable performance by using only a fraction of frequency tones employed by the traditional SFCW radar. Moreover, these frequency tones are transmitted simultaneously using OFDM technology. In the next step research, OFDM-CS GPR circuit hardware will be implemented and tested. Measurement results will be collected and analyzed to examine actual performance and operating speed improvement. Also further study will be conducted to investigate noise effects on OFDM-CS radar data processing.

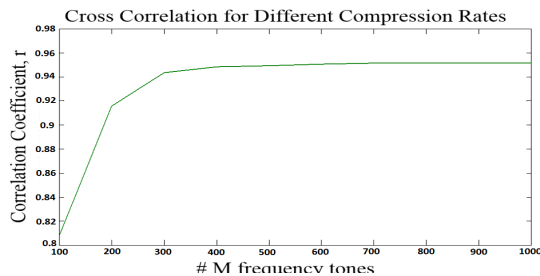


Fig. 7. Cross correlation for different compression ratios

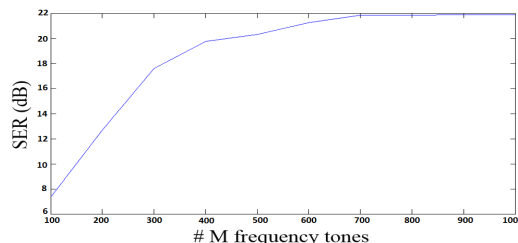


Fig. 8. SER for different compression ratios

References

- [1] T. Xia, X.L. Xu, A. Venkatachalam and D. Huston, "Development of a High Speed UWB GPR for Rebar Detection", *Proceedings of IEEE International Conference on Ground Penetrating Radar (GPR) 2012*.
- [2] A. Venkatachalam, X.L. Xu and D. Huston, T. Xia, "Development of a New High Speed Dual Channel Impulse Ground Penetrating Radar", *IEEE Journal of Selected Topics in Applied Earth Observations and Remote Sensing*, Vol. 6, No. 6, Dec. 2013.
- [3] L. Ying, Q. Zhang, W. Hong, W. YiRong, "Waveform design and high-resolution imaging of cognitive radar based on compressive sensing", *Science China Information Sciences*, 2012.
- [4] A.B. Suksmo, E. Bharata, A.A. Lestari, et. al., "Compressive stepped-frequency continuous-wave ground-penetrating radar", *IEEE Geoscience and Remote Sensing Letters*, 2010, 7(4), 665-669.
- [5] IEEE Standards, 802.11a: <http://standards.ieee.org/getieee802/download/802.11a-1999.pdf>
- [6] M. Metwally, N. L'Esperance, T. Xia, M. Slamani "Continuous Wave Radar Circuitry Testing Using OFDM Technique", 2014 IEEE VLSI Test Symposium.
- [7] D. Donoho, "Compressed sensing," *IEEE Trans. Inf. Theory*, vol. 52, no. 4, 2006. pp. 1289-1306.
- [8] E. Candes, J. Romberg, and T. Tao, "Robust uncertainty principles: Exact signal recovery from highly incomplete information," *IEEE Trans. Inf. Theory*, vol. 52, no. 2, 2006. pp. 489-509.
- [9] E. Candes and J. Romberg, "Sparsity and incoherence in compressive sampling," *Inv. Probl.*, vol. 23, no. 3, 2007. pp. 969-985.
- [10] I. Sarkas, "An Introduction to Compressive Sampling", *IEEE Signal Processing Magazine*. 2008. pp. 21-30.
- [11] T. Xia, R. Shetty, T. Platt, M. Slamani, "Low Cost Time Efficient Multi-tone Test Signal Generation Using OFDM Technique", *Journal of Electronic Testing*, 29(6), 2013. 893-901
- [12] T. Ziani, M. Laour, X. Dérobert, M. Benslama, "2 D simulation with the FDTD method of GPR modelling applied to the detection in stratified lossy medium using the frequency effect pulse", *IEEE International Conference on Electromagnetics in Advanced Applications*, 2009.
- [13] E. J. Candes., "The restricted isometry property and its implications for compressed sensing", *Comptes Rendus Mathematique*, 2008 346(9).
- [14] A. C. Gurbuz, J. H. McClellan, W. R. Scott, "A compressive sensing data acquisition and imaging method for stepped frequency GPRs", *IEEE Trans. on Signal processing*, Vol. 57, No. 7, 2009. pp. 2640-2650.
- [15] X.L. Xu, T. Xia, A. Venkatachalam, and D. Huston, "The Development of A High Speed Ultrawideband Ground Penetrating Radar for Rebar Detection", *ASCE Journal of Engineering Mechanics*, March 2013, Vol. 139, No. 3. pp. 272-285.